Differences in the Binding of Copper(I) to α- and β-Synuclein

(Article begins on next page)

31 July 2024

Differences into the binding of copper(I) to α and β synuclein.

Riccardo De Ricco[‡], Daniela Valensin*[‡], Simone Dell'Acqua[†], Luigi Casella[†], Elena Gaggelli[‡], Gianni Valensin[‡], Luigi Bubacco[§], Stefano Mangani*[‡]

[‡] Department of Biotechnology, Chemistry and Pharmacy University of Siena Via A. Moro 2, Siena, Italy.

[†] Department of Chemistry University of Pavia Via Taramelli 12, Pavia, Italy.

[§] Department of Biology University of Padova Via U. Bassi 58b, Padova, Italy.

ABSTRACT: Parkinson's disease (PD) is a neurodegenerative disorder characterized by the presence of abnormal α-synuclein (αS) deposits in the brain. Alterations in metal- homeostasis and -induced oxidative stress may play a crucial role in the progression of αS amyloid assembly and pathogenesis of PD. Contrary to αS, β-synuclein (βS) is not involved in the PD etiology. However, it has been suggested that the βS : αS ratio is altered in PD, indicating that a correct balance of these two proteins is implicated in the inhibition of αS aggregation. αS and βS share similar abilities to coordinate Cu(II). In this study, we have investigated and compared the interaction of Cu(I) with the N-terminal portion of βS and αS by means of NMR, circular dichroism and X-ray absorption spectroscopies. Our data shows the importance of M10K mutation which induces different Cu(I) chemical environments. A 3S1O and 2S2O coordination modes were identified for βS and αS, respectively. These new insights into the bioinorganic chemistry of copper and Synuclein proteins are a basis to understand the molecular mechanism by which βS might inhibit αS aggregation.

Introduction

Parkinson's disease (PD) is a widespread neurodegenerative pathology associated with severe disorders of the central nervous system mainly caused by the death of dopaminergic cells in the substantia nigra [1-7].

Among several familiar or inherited forms of PD one is linked to the mutation of SNCA genes coding α-synuclein (αS), an intrinsically disordered protein whose biological function is unknown yet. αS is the main component of Lewy bodies, histological hallmark of PD in most inherited, familiar, early-onset and autosomal forms [8-10], which are present in the brains of patients [11, 12].

αS belongs to the Synuclein family, which includes also β- and γ-synuclein (βS and γS, respectively) for their high homologies (62%) in the amino acidic sequence [13]. αS and βS are co-localized in the pre-synaptic nerve terminals mostly expressed in the brain, while γS is found primarily in the peripheral nervous system. [14] Contrary to αS, βS and γS are not correlated to neurodegeneration. Previous studies, have shown that γS is involved in various types of cancer [15-19], while βS, representing 75-80% of the total brain synuclein content, is considered as the non-amyloidogenic homologue of αS [20]. For these reasons, the biological and chemical behavior of βS has been extensively investigated and compared to αS [19, 21].

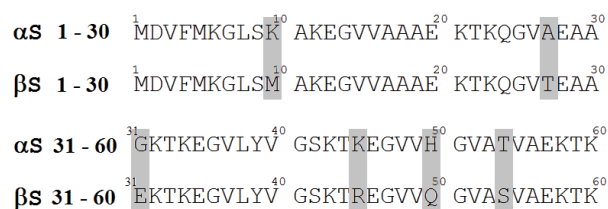In the last few decades, many efforts have been directed to reveal the main cause and the exact mechanisms leading to αS aggregation and their possible implication in PD. Previous intriguing results show that the ratio βS : αS is altered in neurodegenerative disorders, suggesting that a correct balance of these two proteins is implicated in the inhibition of αS aggregation [21-23]. The intrinsic ability of βS to prevent aggregation and oligomerization of αS has been also observed at equimolar protein concentrations. In particular, it has been proposed that the presence of βS gives rise to the formation of αS-βS heterodimers, thus preventing αS homodimerization and oligomerization [24, 25].

Transition metal ions homeostasis (Cu(II)/(I), Fe(III)/(II), Zn(II)) plays a key role in neurodegenerative disorders as they are considered one of the possible factors leading to protein aggregation [26-30]. Moreover, the oxidative stress mediated by redox active metal ions, like copper and iron, is considered to be strictly linked to the production of reactive oxygen species (ROS) strongly implicated in the pathogenesis of PD and other neurodegenerative diseases [31]. In fact, uncontrolled ROS production is one of the most dangerous challenges for cell vitality and is strictly linked with an altered metal homeostasis [31]. Interestingly, altered cellular concentration of metal ions have a significant impact on the development of age-related neurodegenerative diseases [32-34].

The interaction between αS and redox active metal ions has been a topic of numerous investigations. In particular,

it has been shown that (i) αS is able to bind both Cu(II) and Cu(I), (ii) Cu(II) binding has a higher affinity than Cu(I), and (iii) Cu(II) enhances protein aggregation and oligomerization [35-40]. The structural features of the Cu(II) and Cu(I) binding sites have been determined by different experimental methods [38, 41-55] and the existence of two or three possible independent Cu(II) binding domains is widely accepted [28, 38, 41, 42, 49, 47, 52]. The main one (K_d = 0.20 ± 0.02 μM) is located at the N-terminal region, where Cu(II) coordinates to Met-1 N-terminal amino group, Asp-2 main chain nitrogen, Asp-2 carboxylate group and a water molecule or His-50 imidazole [38, 43, 44, 52-56]. The same region is also able to bind Cu(I) with a μM affinity through Met-1 and Met-5 thioether groups [57-59]. Obviously the main Cu(II) binding site anchored to Met-1 amine group is completely abolished if the N-terminus group is acetylated [60].

Recently, Cu(II) binding domains and affinities of αS and βS were compared, showing the occurrence of identical metal binding behavior for both proteins [46]. On the other hand, nothing is known about Cu(I)-βS binding abilities. As easily observed by comparing the amino acid sequences of αS and βS (Scheme 1), the N-terminal region is highly conserved, with the presence of just six point mutations. One is at position 10, where Lys in αS is substituted by Met in βS. Since methionine residues constitute the Cu(I) binding domain, K10M substitution might provide a new possible thioether ligand for Cu(I) in βS. The presence of an additional methionine residue in the protein sequence, could have a strong impact on the copper(I) coordination environment and binding affinity of βS, in contrast to what was observed for Cu(II) binding [46].

αS 1 - 30   MDVFMKGLSK AKEGVVAAAE KTKQGVAEAA

βS 1 - 30   MDVFMKGLSM AKEGVVAAAE KTKQGVTEAA

αS 31 - 60   GKTKEGVLYV GSKTKEGVVH GVATVAEKTK

βS 31 - 60   EKTKEGVLYV GSKTREGVVQ GVASVAEKTK

Scheme 1. Comparison of the N-terminal sequences (1-60) of α- and β-synuclein. The six single point mutations are shown in gray (K10M, A27T, G31E, K45R, H50Q and T54S.

In order to address this issue, here we investigated the behavior of the N-terminal region of βS in presence of Cu(I) by means of NMR, CD, and XAS spectroscopies. The complete characterization of the metal coordination site and the 3D structure of the complex was obtained by using the peptide encompassing the first 15 amino acids (βS$_{1-15}$) which, as previously shown for αS, represents a good model for the copper binding at the N-terminal region of the full length protein [37, 41, 46, 58-61].

In addition to Cu(I), we also investigated Ag(I)-βS$_{1-15}$ interaction by NMR spectroscopy in order to evaluate whether silver can act as a good probe of the Cu(I)-synuclein associations [62]

Experimental Section

Peptides and reagents - The N-terminal βS$_{1-15}$ and αS$_{1-15}$ peptides were synthesized in solid phase using Fmoc chemistry. Rink-amide resin was used as the solid support, so that the resulting peptides are amidated at the C-terminus. After removal of the peptide from the resin and deprotection, the crude product was purified by RP HPLC on a Phenomenex Jupiter Proteo C12 column, using a Jasco PU-1580 instrument with diode array detection (Jasco MD-1510), with a semi-linear gradient of 0.1% trifluoroacetic acid (TFA) in water to 0.1% TFA in CH_3CN over 40 min. The identity of the peptide was confirmed by Electrospray ionization mass spectrometry (Thermo-Finnigan). The purified peptide was lyophilized and stored at -20 °C until use. βS$_{1-15}$ and αS$_{1-15}$ were dissolved in 20 mM or 2 mM phosphate buffer in H_2O at pH 7.3, obtaining a final concentration ranging from 400 to 500 μM for NMR experiments, 100 μM for CD experiments and 1.0 mM for XAS experiments. The desired concentration of Ag(I) ions was achieved by using a stock solution of 20 mM $AgNO_3$ (Sigma Chemical Co.) in D_2O. For Cu(I) complexes 10 mM $[Cu(CH_3CN)_4]BF_4$ stock solution was prepared in 20 mM phosphate buffer in D_2O at pH 7.3 containing 5% v/v CH_3CN. Ascorbic acid was added to the peptides (ratio 2:1) just before use in order to avoid any possible oxidation of Cu(I) to Cu(II). All the solutions were degassed with water-saturated N_2 just before use and kept under inert N_2 atmosphere. TMSP-2,2,3,3-d$_4$, 3-(trimethylsilyl)-[2,2,3,3-d$_4$] propansulfonate, sodium salt, was used as internal reference standard for NMR measurements.

CD measurements - CD spectra were acquired on a Jasco J-815 spectropolarimeter at 288 K. A 0.1 cm cell path length was used for data between 180 and 260 nm, with a 1 nm sampling interval. Four scans were collected for every sample with scan speed of 100 nm min^{-1} and bandwidth of 1 nm. Baseline spectra were subtracted from each spectrum and data were smoothed with the Savitzky-Golay method [63]. Data were processed using Origin 5.0 spread sheet/graph package. The direct CD measurements (θ, in millidegrees) were converted to mean residue molar ellipticity, using the relationship mean residue Δε = θ /(33000×c×l×number of residues), where c and l refer to molar concentration and cell path length respectively.

NMR measurements - NMR spectra were acquired at 278 and 288 K using Bruker Advance spectrometer operating at proton frequency of 600 MHz. NMR spectra were processed with XwinNMR 3.6 and TopSpin 2.0 software and analyzed with the program Cara [64]. Suppression of residual water signal was achieved either by presaturation or by excitation sculpting [65], using a selective 2 ms long square pulse on water. Proton resonance assignment of the peptides was obtained by 2D ^{1}H-^{1}H COSY, TOCSY and NOESY and ^{1}H-^{13}C HSQC experiments were performed.

XAS measurements - The Cu(I) αS$_{1-15}$ and βS$_{1-15}$ samples for XAS measurements consisted of 1 mM peptide solutions in 20 mM phosphate buffer at pH 7.3 ± 0.1 1 and were prepared under nitrogen atmosphere by adding Cu(I) in slightly substechiometric ratio to avoid unbound metal (~ 0.9 mM). A glove box under inert atmosphere

was used to load the peptide sample into a plastic cell covered with Kapton windows. The sample holder and the Kapton windows had been previously carefully washed with a highly concentrated EDTA solution (approx. 100 mM), rinsed with pure water, absolute ethanol and dried. The sample cell was then mounted in a cryostat and kept at 100 K during data collection. XAS data were collected at the GILDA CRG beamline of the European Synchrotron Radiation Facility (Grenoble, France), using a Si(311) double-crystal monochromator employing dynamical sagittal focusing [66]. The photon flux was of the order of 10^{10} photons s^{-1} and 1 mm x 1 mm spot size. The XAS data were recorded by measuring the Cu-K$_\alpha$ fluorescence using a Ge 12-element solid-state detector over the energy range from 8800 to 9600 eV, using variable energy step widths. In the X-ray absorption near-edge structure (XANES) and extended X-ray absorption fine structure (EXAFS) regions steps of 0.5 and 2.0 eV were used, respectively. Ionization chambers in front and behind the sample were used to monitor the beam intensity. Energy calibration of the spectra was obtained by measuring metallic Cu foil. Data reduction to extract the EXAFS spectrum was performed with the Athena software package [67]. The full, k^3 weighted, EXAFS spectra (20-790 eV above E_o = 8983.9 eV) and their Fourier transforms (FT) calculated over the range 3.0-14.0 Å^{-1} have been compared with theoretical simulations obtained by utilizing the rapid curved multiple scattering theory implemented in the set of programs EXCURVE9.20 [68, 69] The quality of the fit was assessed by the goodness of fit function through the parameter ε^2 which accounts for the degree of over-determinacy [70] and by the R-factor as defined within EXCURVE9.20 [68, 69].

Structure determination - NOE cross peaks in 2D ^{1}H-^{1}H NOESY spectra acquired on Cu(I)-βS$_{1-15}$ and Ag(I)-βS$_{1-15}$ complexes at 278 K were integrated with Cara program and were converted into upper internuclear distances with the routine CALIBA of the program package DYANA [71]. The intra- and inter-residue constraints obtained were used to generate an ensemble of 30 structures by the standard protocol of simulated annealing in torsion angle space implemented in DYANA (using 10000 steps). To take into account the observed coordination behaviour of silver, distance constraints between metal and the three sulfur methionine were imposed. No dihedral angle restraints and no hydrogen bond restraints were applied. The final structures were analyzed using the program MOLMOL [72].

Results

βS$_{1-15}$-*Cu(I) binding* – NMR and XAS spectroscopies were used to investigate the copper(I) coordination sphere of βS$_{1-15}$. Upon Cu(I) addition, chemical shift variations on selected NMR resonances were observed by comparing ^{1}H–^{13}C HSQC NMR spectra of the apo and the metal bound βS$_{1-15}$ (Figure 1A). The most affected signals belong to ε-CH$_3$ and γ-CH$_2$ groups of Met-1, Met-5 and Met-10, which showed about 0.2 and 3.0 ppm downfield

shifts for ^{1}H and ^{13}C resonances respectively. Aside Met residues, significant chemical shift perturbations were also observed for Asp-2, Val-3 and Phe-4 correlations. The same ^{1}H–^{13}C HSQC NMR spectra were additionally recorded in presence of 0.9 Ag(I) equiv. in order to compare the behavior of the two metal ions. As easily observed in Figure 1, Ag(I) causes almost identical chemical shift variations on NMR resonances of βS$_{1-15}$ thus suggesting the involvement of the same binding donors in the two metal coordination spheres.

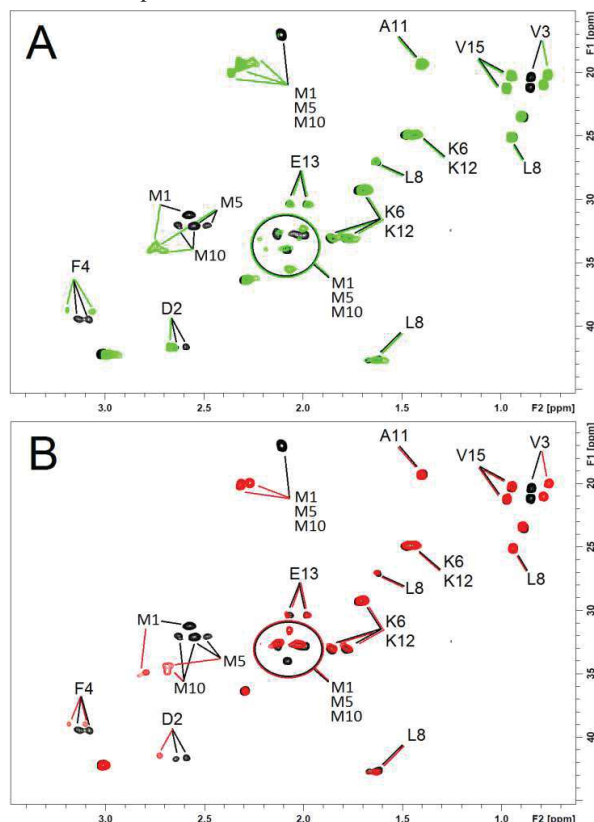Figure 1. ^{1}H–^{13}C HSQC NMR spectra of βS1-15 in the absence (black contours) and in the presence of: A. 0.9 equiv. of Cu(I) (green contours); B. 0.9 equiv. of Ag(I) (red contours). The peptides (0.50 mM) was dissolved in H2O:D2O 90:10, 20 mM phosphate buffer, pH 7.3 at 288 K.

Additional features of the Ag(I)/Cu(I) coordination sites were obtained comparing the ^{1}H-^{1}H TOCSY spectra of the apo and the bound βS$_{1-15}$ forms. The chemical shift variations measured in the presence of 0.9 Cu(I) equiv., are shown in Figure 2A. Beside the large effects detected on Met-1, Met-5 and Met-10, the backbone protons of the first 6 amino acids and of Leu-8 and Ser-9 are also affected by the metal ion. On the other hand, the C-terminal region (11-15) exhibits negligible changes. Figure 2A also illustrates that Met residues only, show relevant shifts on side-chain protons (Hγ, Hε), clearly indicating the three sulfur atoms as the copper(I) anchoring site. The presence of 0.9 equiv. of Ag(I) ions yields changes on Hα resonances almost identical to the ones recorded for Cu(I), con-

firming the occurrence of similar binding mode for both Ag(I) and Cu(I) (Figure 2B).

In order to better identify the role played by Met-10, we compared the 2D NMR spectra of αS_{1-15} and βS_{1-15} recorded in presence of 0.9 Ag(I) equiv. (Figure 1S). As easily observed, the two peptides possess very similar NMR spectra with the obvious exception of Met/Lys mutation.
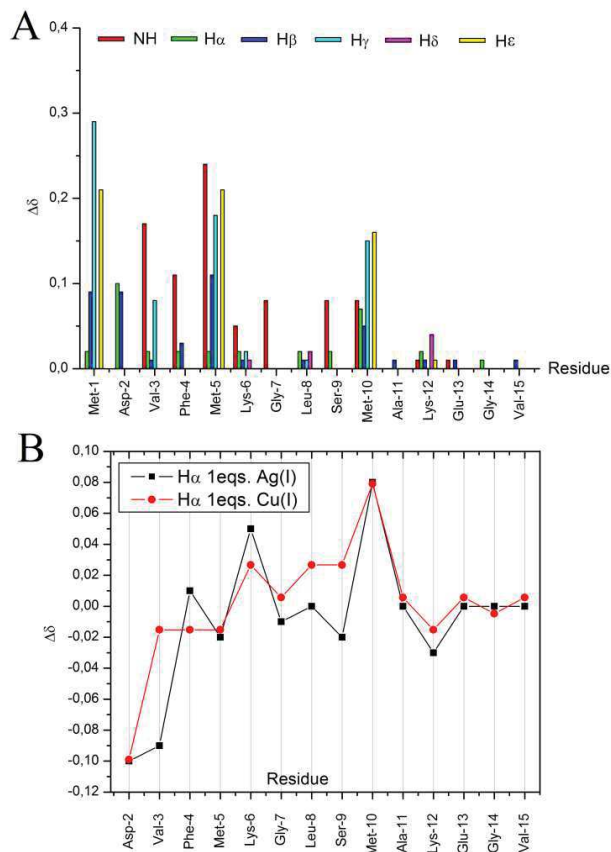

Figure 2. A. Chemical shift variations ($\Delta\delta = \delta$bound – δapo) of βS_{1-15} 0.40 mM at 288 K in the presence of 0.9 equiv of Cu(I). B. Comparison between Hα chemical shift variations of βS_{1-15} induced by the presence of 0.9 equiv of Cu(I) (red) and Ag(I) (black) ions.

In addition to NMR, XAS spectra of both Cu(I)-βS_{1-15} and Cu(I)-αS_{1-15} complexes were measured at the Cu K-edge to better identify the first copper(I) coordination shell of βS_{1-15} and compare it with that of αS_{1-15}. The Cu K-edge XANES regions of Cu(I)-αS_{1-15} and Cu(I)-βS_{1-15} complexes are reported in Figure 3. The experimental EXAFS spectra, the Fourier filtered spectra and the Fourier Transforms (FT), together with the best fits for the two peptides, are reported in Figures 4a-f respectively.

The Cu-Kα edges of both samples are characteristic of Cu(I) compounds both located at 8980 eV and showing a quite sharp 1s-4p transition at 8982 eV. However, the two edges differ at the edge peak and in the XANES region indicating the occurrence of different chemical environments for the two Cu(I) ions. The intensity and sharpness of the 1s-4p peak decreases from linearly two-coordinated

Cu(I) sites to tetrahedral ones, although other factors, like distortions from ideal geometry influence the transition intensities [73]. When compared to the model compounds reported in the literature [74-78], this feature appears very similar, in both samples, to the transition present in tri- or four-coordinated Cu(I) centers containing sulfur coordination.
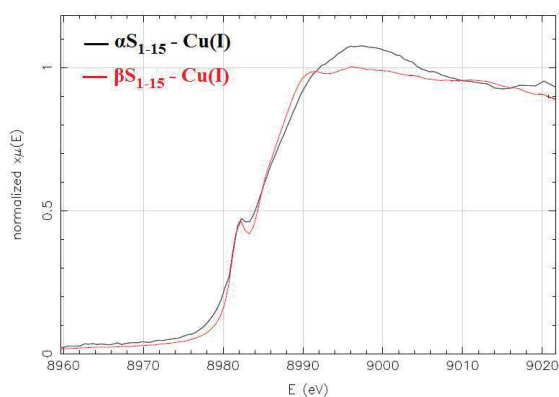

Figure 3. XANES region of Cu(I) complexes with αS (black line) and βS (red line) peptides. Alignment of the 1s-4p transition at 8982 eV is visible.

The quality of the data is not outstanding, however, the signal/noise ratio is satisfactory up to about k = 12.5 Å^{-1}, allowing the extraction of useful structural information from the spectrum concerning the Cu(I) first coordination shell. To this purpose we have used Fourier filtering to isolate the spectrum contributions up to about 2.8 Å. Figures 4e and 4f show the FT of the filtered data for the two samples. The FT for αS_{1-15}-Cu(I) reveals the occurrence of two resolved ligand shells (at ~1.9 Å and 2.3 Å), while the Cu(I) coordination environment in βS_{1-15} appears to be dominated by sulfur ligation. Similar data were obtained by analyzing the FT of the raw data (without filtering) thus excluding the presence of artefacts due to Fourier filtering (Figure 2S). Different fits of the EXAFS and FTs have been performed for both samples, varying the number of ligand shells from 2 to 4 with all possible combinations of O/N and S ligands and coordination numbers (as integers) summing up to 3 or 4. Table 1 reports the structural parameters relative to the copper coordination obtained from the best fits to the spectra of the two samples, while the parameters obtained by fitting the EXAFS and FTs by varying the shell number and the coordinated atoms are shown in Table 1S. It can be noticed that the best fits were obtained by using only two shells of ligands as increasing the number of shells did not significantly improved the fits. These results indicate the existence of a quite homogeneous Cu(I) environment in both samples with low static disorder as confirmed by the low values of the Debye-Waller parameters. The theoretical fits match the experimental data quite well (Figure 4c-f) and support the existence of different coordination environments for Cu(I) in αS_{1-15} and βS_{1-15}. The first shell of Cu(I)-αS_{1-15} is clearly split into two contributions at different distances. The analysis of the EXAFS spectrum of Cu(I)-αS_{1-15} indi-

cates a four coordinated Cu(I) ion bound to two O/N atoms at 1.94 Å, and 2 S ligands at 2.35 Å. The short Cu-O/N distances is compatible with the possible binding of carboxylate and or amide nitrogen ligands. The two sulphur ligands belong to methionine residues. The Cu(I)-βS_{1-15} EXAFS spectrum displays quite different features with respect to the α-peptide. The first shell contributions are not so well defined as for Cu(I)-αS_{1-15} indicating smaller contribution from O/N donors with respect to S donors. The fitting results in one O/N ligand at about 1.95 Å, three sulfur ligands at 2.29 Å.
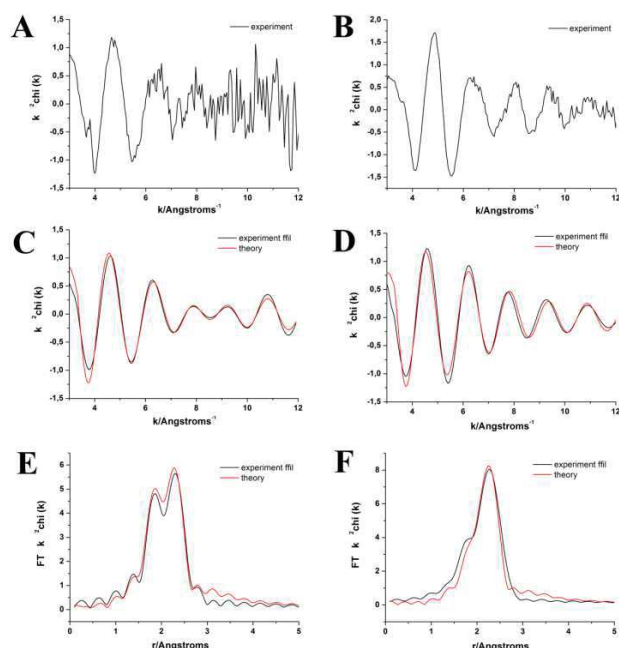
Figure 4. Comparison of the theoretical signal (red) with experimental data (black) of Cu K-edge XAS spectra of copper(I) complexes of αS_{1-15} and βS_{1-15}. k^2-weighted EXAFS data of (A) Cu(I)–αS_{1-15} and (B) Cu(I)–βS_{1-15}. k^2-weighted EXAFS data filtered to remove the residue noise of (C) Cu(I)–αS_{1-15} and (D) Cu(I)–βS_{1-15}. Fourier transforms of (E) Cu(I)–αS_{1-15} and (F) Cu(I)–βS_{1-15}.

Table 1. Structural Parameters of Cu(I) binding to αS_{1-15} and βS_{1-15}

Sample	R-factor	Atom type	Distance (Å)	Debye–Waller factor (2σ) (Å2)	N° shell
Cu(I) –αS_{1-15}	18.84	2O/N	1.924	0.0029	2
		2S	2.294	0.0055	
Cu(I) –βS_{1-15}	22.48	1O/N	1.950	0.0032	2
		3S	2.295	0.0073	

Structural details of Cu(I)-βS_{1-15} complex - In order to preliminarily monitor the conformational propensities of βS_{1-15} in presence and in absence of metal ions, CD spectra of apo and silver bound peptides were collected (Figure

5). The CD spectrum of apo βS_{1-15} shows the typical random coil absorption band at 198 nm. The addition of increasing amounts of Ag(I) in solution (from 0.125 up to 4 equiv.) does not result in any shift of the amide bonds transitions (Figure 5, colored dashed lines), but it yields a decreased in intensity of the transition.
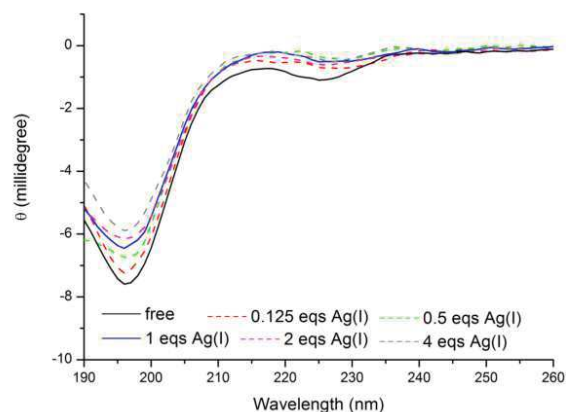
Figure 5. CD spectra of βS_{1-15}. Black (apo peptide); red (0.125 Ag(I) equiv); gree (0.500 Ag(I) equiv); blue (1.00 Ag(I) equiv); magenta (2.00 Ag(I) equiv); gray (4.00 Ag(I) equiv).

Additional metal-induced conformational details were determined by integrating the NOEs correlations of ^1H -^1H NOESY spectra of both Cu(I)-βS_{1-15} and Ag(I)-βS_{1-15} complexes. The measured integrals were then used to obtain a set of inter- and intra-residue proton-proton distances, to be used, together with the Cu(I)-S distances derived from the EXAFS fitting (Table 1), as restraints for the calculation of the 3D structures.

As reported in Figures 1 and 2, Cu(I) and Ag(I) complexes with βS_{1-15} exhibit very similar NMR behavior. However, all the NMR spectra acquired in the presence of Cu(I) were characterized by a huge line broadening of Met-1, probably due to the presence of small amount of oxidized Cu(II) bound to the N-terminal amino group. For these reasons, only the ^1H-^1H distances derived from Ag(I)-βS_{1-15} interaction were used for structure calculation. The obtained first 15 structures are reported in Figure 6A, showing a good superimposition of the N-terminal region only (1-5 residues).

Among the three methionines, Met-5 possesses a fix and stable side-chain orientation, while the thioether groups of Met-1 (yellow spheres) and Met-10 (green spheres) are more flexible, experiencing different relative positions. This might be due to the lack of NMR constraints which prevent to unequivocally determine Met-1 and Met-10 positions. As shown in Figure 6, the absence of NOEs constraints also yields a general disorder for all the C-terminal region. Interestingly, the carboxylic group of Asp-2 (red spheres) is in close proximity to the metal coordination sphere for all the 30 calculated structures (2.50 Å), strongly suggesting its interaction with the metal ion. For these reasons, a second structure calculation was performed by further adding the Cu(I) Asp-2 carboxylate binding distance (1.95 Å), as additional constraint. The

best 15 structures (Figure 6B) show an improved structural resolution and a better defined metal coordination sphere. This approach, combining NMR and XAS investigations, provides structural details of both the protein conformation and the metal site as previously illustrated for the structure determination of bacterial copper transport proteins [79].
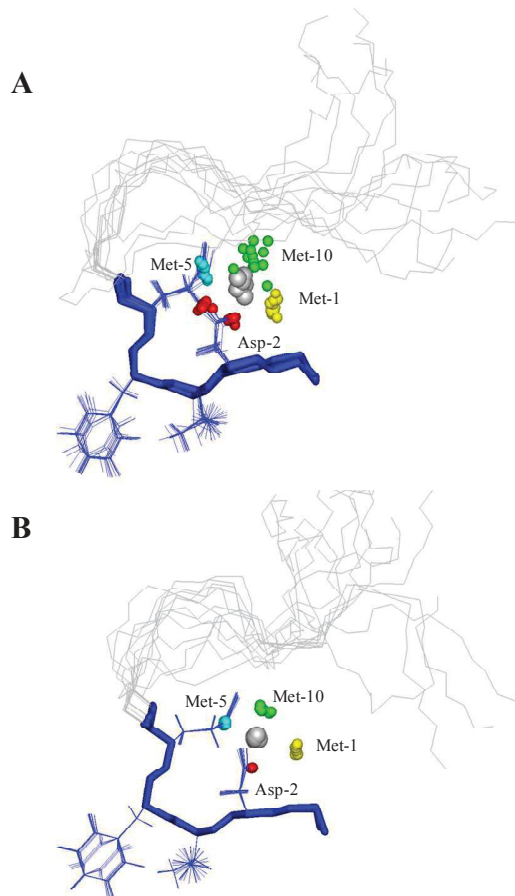

Figure 6. Superimposition of the first 15 structures obtained for the Ag(I)-βS1-15 complex calculated without (A) and with (B) the binding of Asp-2 carboxylate. The structures are fitted on the 1-5 backbone residues with RMSD values for the backbone atoms 0.29 ± 0.12 and 0.14 ± 0.08 Å for A and B respectively. The sulfur donor atoms of Met-1, Met-5 and Met-10 are shown as yellow, cyan and green spheres, respectively. The carboxylic oxygen atoms of Asp-2 are shown as red spheres and the silver ion is shown as a grey sphere. Figure was created with MOLMOL 2K.1.0

Discussion

The interactions between amyloidogenic proteins and transition metal ions have been widely investigated in the last decades [26-30]. It is well accepted that, Aβ, αS and PrP, the misfolded proteins correlated to Alzheimer, Parkinson and Prion diseases respectively, share the ability to bind copper in both its oxidation states. In addition, it has been shown that Cu(II)/Cu(I) binding to αS and Aβ affects both protein aggregation and the production of reactive oxygen species *in vitro* [36-42].

For these reasons, many efforts have been directed to understand the structural features of copper complexes with αS and Aβ [see reviews 61, 62, 80]. The existence of multiple metal binding modes, in equilibrium and simultaneously present in solution, is usually observed for most of the cases. This is probably due to the absence of particular protein fold stabilizing specific metal binding sites.

Previous investigations have shown that the N–terminal region of αS is able to bind Cu(II) and Cu(I) ions [38, 43-58]. The anchoring site of the cupric ion is the Met-1 amino group which gives rise to the formation of a stable metal coordination sphere involving the amide nitrogen and the carboxylate oxygen atoms belonging to Asp-2 as well [28, 38, 43, 45, 52-56]. As expected, the latter binding mode is completely absent in acetylated αS [60]. Like αS, βS is able to bind Cu(II) at the N-terminus, between residues 1-9 [41]. The resulting Cu(II) complex is very similar to the one detected for βS in agreement with the fact that the two proteins contain several identical amino acids in the region 1-9 (Scheme 1).

Conversely, Cu(I) binding donor atoms in αS and βS are provided by thioether groups of Met which might act as metal anchoring sites for acetylated αS as well. βS has an additional Met at position 10 which strongly impacts the Cu(I) binding abilities of this protein. Our NMR findings clearly indicate that Met-1, Met-5 and Met-10 of βS interact with the metal ion (Figure 1A). In addition, XAS analysis have provided evidence of different Cu(I) chemical environment for Cu(I)-αS$_{1-15}$ and Cu(I)-βS$_{1-15}$ complexes (Figure 3). Such behavior is also evident by looking at the structural parameters calculated from the fitting of the EXAFS spectra and reported in Table 1, which reveal Cu(I) coordination to 2S and 3S atoms for αS$_{1-15}$ and βS$_{1-15}$, respectively. The key role played by Met residues in stabilizing the metal coordination sphere is also supported by a recent study showing that Met/Ile substitution in αS leads to dramatic decrease of Cu(I)-αS affinity [81].

In addition to the participation of 2/3 sulfur atoms, EXAFS investigation revealed that 2 and 1 O/N atoms complete the metal coordination sphere for αS and βS, respectively, thus indicating the presence of four-coordinated Cu(I) ion, probably with a tetrahedral geometry. The oxygen atoms might be derived from water molecules or carboxylate groups belonging to Asp and Glu, which usually take part in metal-protein complexation. On the other hand nitrogen atoms might be provided by amino N-terminal group or acetonitrile. By looking at the ¹H chemical shift variations induced by the metal (Figure 2), with the exception of the changes observed on all the three Met, Asp-2 is the only residue exhibiting significant effects on both Hβ and Hα thus supporting its binding to Cu(I) for both αS and βS systems. In fact, Asp-2 chemical variations were also detected for αS$_{1-6}$ and αS$_{1-15}$ systems in the presence of Cu(I) and Ag(I), respectively [46, 58]. However, their smaller values compared to the ones observed for Met (~ 0.06 *vs* ~ 0.2 ppm) lead to exclude the involvement of Asp-2 in Cu(I) binding [73, 74]. The involvement of Asp-2 is also supported by the structural calculation reported in Figure 6, showing that the carbox-

ylate group is nicely approaching the metal ion in all the 30 derived structures. Interestingly, the participation of Asp-2 in both Cu(II) and Cu(I) binding represent the unique common element between the coordination spheres of the two metal ions, which experience different donor atoms (N *vs* S) in Cu(II) and Cu(I) oxidation states respectively.

Previous NMR investigations excluded the interaction of Asp-2 probably because of the smaller effects observed on its protons compared to the ones measured for Met residues (~ 0.06 *vs* ~ 0.2 ppm) [46, 58].

With regard to the additional oxygen/nitrogen atom bound to Cu(I) in αS_{1-15} system only, it probably belong to a water or acetonitrile molecule . In fact, this and previous NMR investigations [46, 58] indicate that no other residues experience such chemical shift variations to support their coordination to the metal ion.

In conclusion our findings point out that the N-terminal regions of αS and βS interact differently with the cupreous ion, conversely to what previously reported for Cu(II) [41]. In fact, while Cu(II) binding sites are well conserved in αS and βS, different donor atoms are involved in the Cu(I) coordination sphere of the two proteins. The main difference is due to M10K point mutation which leads to different coordination modes: 2S2O and 3S1O in αS and βS, respectively. These differences might influence the biological behavior of the two proteins and in particular their redox features. We indeed expect that some significant change in redox properties of copper complexes of αS and βS will occur by virtue of the difference in coordination set of their Cu(I) forms, assuming that their Cu(II) counterparts bear the same coordination environment. The reduced state should be more easily accessible for Cu-βS than Cu-αS, and therefore we expect a higher redox potential for the Cu(II)/Cu(I) couple of βS than αS.

ASSOCIATED CONTENT

A Table showing the structural parameters of Cu(I) binding to αS_{1-15} and βS_{1-15} derived from different fits of the EXAFS and FTs (Table 1S); a superimposition of 2D NMR TOCSY spectra of αS_{1-15} and βS_{1-15} in presence of 0.9 eqs. of Ag(I) (Figure 1S); comparison of the Fourier Transform of the experimental and the theoretical signal of the Cu K-edge XAS spectra of copper(I) complexes of αS_{1-15} and βS_{1-15} (Figure 2S) are shown in Supporting Information. This material is available free of charge via the Internet at http://pubs.acs.org.

AUTHOR INFORMATION

Author Contributions

The manuscript was written through contributions of all authors. All authors have given approval to the final version of the manuscript.

REFERENCES

[1] Conway, K. A.; Lee, S. - J.; Rochet, L. - C.; Ding, T. T.; Williamson, R. E.; Lansbury, P. T. *Prot. Natl. Acad. Sci.* **2000**, *97*, 571-576.

[2] Bucciantini, M.; Giannoni, E.; Chiti, F.; Baroni, F.; Formigli, L.; Zurdo, J.; Taddei, N.; Ramponi, G.; Dobson, C. M.; Stefani, M. *Nature* **2002**, *416*, 507-511.

[3] Kayed, R.; Head, E.; Thompson, J. L.; McIntire, T. M.; Milton, S. C.; Cotman, C. W.; Glabe, C. G. *Science* **2003**, *300*, 486-489.

[4] Danzer, K. M.; Haasen, D.; Karow, A. R.; Moussaud, S.; Habeck, M.; Giese, A.; Kretzschmar, H.; Hengerer, B.; Kostka, M. J. *Neurosci.* **2007**, *27*, 9220-9232.

[5] Winner, B.; Jappelli, R.; Maji, S. K.; Desplats, P. A.; Boyer, L.; Aigner, S.; Hetzer, C.; Loher, T.; Vilar, M. A.; Campioni, S.; Tzitzilonis, C.; Soragni, A.; Jessberger, S.; Mira, H.; Consiglio, A.; Pham, E.; Masliah, E.; Gage, F. H.; Riek, R. *Proc. Natl. Acad. Sci.* **2011**, *108*, 4194-4199.

[6] Gurry, T.; Ullman, O.; Fisher, C. K.; Perovic, I.; Pochapsky, T.; Stultz, C. M. *J. Am. Chem. Soc.* **2013**, *135*, 3865–3872.

[7] Pivato, M.; De Franceschi, G.; Tosatto, L.; Frare, E.; Kumar, D.; Aioanei, D.; Brucale, M.; Tessari, I.; Bisaglia, M.; Samori, B.; Polverino De Laureto, P.; Bubacco, L. *PlosONE* **2012**, *7*, e50027.

[8] Bisaglia, M.; Mammi, S.; Bubacco, L. *FASEB* **2009**, *23*, 329–340.

[9] Yoon, J.; Jang, S.; Lee, K.; Shin, S. *J. Biomol. Struct. Dyn.* **2009**, *27*, 259–270.

[10] Brown, D.R. *FEBSJ* **2007**, *274*, 3766-3774.

[11] Goedert, M. *Nat. Rev. Neurosci.* **2001**, *2* 492-501.

[12] Spillantini, M. G.; Schmidt, M. L.; Lee, V. M.; Trojanowski, J. Q.; Jakes, R.; Goedert, M. *Nature* **1997**, *388*, 839-840.

[13] Clayton, D. F.; George, J. M. *Trends Neurosci.* **1998**, *21*, 249–254.

[14] Buchman, V. L.; Hunter, H. J.; Pinon, L. G.; Thompson, J.; Privalova, E. M.; Ninkina, N. N.; Davies, A. M. *J. Neurosci.* **1998**, *18*, 9335–9341.

[15] Tongli, J.; Yiliang, E. L.; Jingwen, L.; Shi, Y. E. *CancerResearch* **1999**, *59*, 742–747.

[16] Ahmad, M.; Attoub, S.; Singh, M. N.; Martin, F. L.; El-Agnaf. O. M. A. *FASEB J.* **2007**, *21* 3419-3430.

[17] Ye, Q.; Huang, F.; Wang, X. – Y.; Xu, Y. – M.; Gong, F. – S.; Huang, L. – J.; Yang, C. – K.; Zheng, Q. –H.; Ying, M. – G. *OncologyReports* **2013**, *30*, 2161-2170.

[18] Wu, K.; Quan, Z.; Weng, Z.; Li, F.; Zhang, Y.; Yao, X.; Chen, Y.; Budman, D.; Goldberg, I. D.; Shi, Y. E. *Breast Cancer Res. Treat.* **2007**, *101*, 259–267.

[19] Bertoncini, C. W.; Rasia, R. M.; Lamberto, G. R.; Binolfi, A.; Zweckstetter, M.; Griesinger, C.; Fernandez, C. O. *J. Mol. Biol.* **2007**, *372*, 708–722.

[20] Uversky, V.N.; Li, J.; Souillac, P.; Millett, I.S.; Doniach, S.; Jakes, R.; Goedert, M.; Fink, A. L. *J. Biol. Chem.* **2002**, *277*, 11970–11978.

[21] Rockenstein, E.; Hansen, L. A.; Mallory, M.; Trojanowski, J. Q.; Galasko, D.; Masliah, E. *Brain Res.* **2001**, *914*, 48–56.

[22] Masliah, E.; Rockenstein, E.; Veinbergs, I.; Sagara, Y.; Mallory, M.; Hashimoto, M.; Mucke, L. *Proc. Natl. Acad. Sci.* **2001**, *98*, 12245–12250.

[23] Rochet, J. C.; Conway, K. A.; Lansbury, P. T. *Biochemistry* **2000**, *39*, 10619–10626.

[24] Hashimoto, M.; Rockenstein, E.; Mante, M.; Mallory, M.; Masliah, E. *Neuron* **2001**, *32*, 213–223.

[25] Masliah, E.; Hashimoto, M. *NeuroToxicology* **2002**, *23*, 461–468.

[26] Bharathi; Indi, S. S.; Rao, K. S. J. *Neurosci. Lett.* **2007**, *424*, 78–82.

[27] Brown, D. R. *Metallomics* **2011**, *3*, 226-228.

[28] Davies, P.; Wang, X.; Sarell, C. J.; Drewett, A.; Marken, F.; Viles, J. H.; Brown, D. R. *Biochemistry* **2011**, *50*, 37-47.

[29] Wang, X.; Moualla, D.; Wright, J. A.; Brown, D. R. *J. Neurochem.* **2010**, *113*, 704–714.

[30] Wright, J. A.; Wang, X.; Brown. D. R. *FASEB J.* **2009**, *23*, 2384-2393.

[31] Kozlowski, H.; Luczkowski, M.; Remelli, M.; Valensin, D. *Coord. Chem. Rev.* **2012**, 256, 2129-2141.

[32] Allsop, D.; Mayes, J.; Moore, S.; Masad, A.; Tabner, B. J. *J. Biochem. Soc. Trans.* **2008**, *36*, 1293–1298.

[33] Lovell, M. A. *J. Alzheimers Dis.* **2009**, *16*, 471–483.

[34] Bolognin, S.; Messori, L.; Zatta, P. *Neuromol. Med.* **2009**, *11*, 223–238.

[35] Paik, S. R.; Shin, H. - J.; Lee, J. - H.; Chang, C. - S.; Kim, J. *Biochem. J.* **1999**, *340*, 821-828.

[36] Macomber, L.; Imlay, J. A. *Proc. Natl. Acad. Sci.* **2009**, *106*, 8344–8349.

[37] Binolfi, A.; Rodriguez, E. E.; Valensin, D.; D'Amelio, N.; Ippoliti, E.; Obal, G.; Duran, R.; Magistrato, A.; Pritsch, O.; Zweckstetter, M.; Valensin, G.; Carloni, P.; Quintanar, L.; Griesinger, C.; Fernandez, C. O. *Inorg. Chem.* **2010**, *49*, 10668–10679.

[38] Binolfi, A.; Quintanar, L.; Bertoncini, C. W.; Griesinger, C.; Fernandez, C. O. *Coord. Chem. Rev.* **2012**, 256, 2188-2201.

[39] Hong, L.; Simon, J. D. *J. Phys. Chem. B* **2009**, *113*, 9551–9561.

[40] Wang, C.; Liu, L.; Zhang, L.; Peng, Y.; Zhou, F. *Biochemistry* **2010**, *49*, 8134–8142.

[41] Binolfi, A.; Lamberto, G.R.; Duran, R.; Quintanar, L.; Bertoncini, C.W.; Souza, J.M.; Cerveñansky, C.; Zweckstetter, M.; Griesinger, C.; Fernàndez, C.O. *J. Am. Chem. Soc.* **2008**, *130*, 11801-11812.

[42] Drew, S. C.; Leong, S. L.; Pham, C. L.; Tew, D. J.; Masters, C. L.; Miles, L. A.; Cappai, R.; Barnham, K. J. *J. Am. Chem. Soc.* **2008**, *130*, 7766–7773.

[43] Kowalik-Jankowska, T.; Rajewska, A.; Wisniewska, K.; Grzonka, Z.; Jezierska, J. *J. Inorg. Biochem.* **2005**, *99*, 2282-2291.

[44] Dudzik, C. G.; Walter, E. D.; Millhauser, G. L. *Biochemistry* **2011**, *50*, 1771-1777.

[45] Bortolus, M.; Bisaglia, M.; Zoleo, A.; Fittipaldi, M.; Benfatto, M.; Bubacco, L.; Maniero, A. L. *J. Am. Chem. Soc.* **2010**, *132*, 18057-18066.

[46] Binolfi, A.; Valiente-Gabioud, A. A.; Duran, R.; Zweckstetter, M.; Griesinger, C.; Fernandez, C. O. *J. Am. Chem. Soc.* **2011**, *133*, 194-196.

[47] Valensin, D.; Camponeschi, F.; Luczowsky, M.; Baratto, M. C.; Remelli, M.; Valensin, G.; Kozlowski, H. *Metallomics* **2011**, *3*, 292-302.

[48] Hong, L.; Simon, J. D. *Metallomics* **2011**, *3*, 262-266.

[49] Lucas, H. R.; DeBeer, S.; Hong, M. – S.; Lee, J. C. *J. Am. Chem. Soc.* **2010**, *132*, 6636-6637.

[50] Faller, P.; Hureau, C.; Dorlet, P.; Hellwig, P.; Coppel, Y.; Collin, F.; Alies, B. *Coord. Chem. Rev.* **2012**, *256*, 2381-2396.

[51] Bruno, A.; Renaglia, E.; Rozga, M.; Bal, W.; Faller, P.; Hureau, C. *Anal. Chem.* **2013**, *85*, 1501-1508.

[52] Rasia, R. M.; Bertoncini, C. W.; Marsh, D.; Hoyer, W.; Cherny, D.; Zweckstetter, M.; Griesinger, C.; Jovin, T. M.; Fernandez, C. O. *Prot. Natl. Am. Soc.* **2005**, *102*, 4294-4299.

[53] Hong, L.; Simon, J. D. *J. Phys. Chem. B* **2009**, *113*, 9551-9561.

[54] Drew, S. C.; Leong, S. L.; Pham, C. L.; Tew, D. J.; Masters, C. L.; Miles, L. A.; Cappai, R.; Barnham, K. J. *J. Am. Chem. Soc.* **2008**, *130*, 7766–7773.

[55] Kowalik-Jankowska, T.; Rajewska, A.; Jankowska, E.; Grzonka, Z. *Dalton Trans.* **2006**, *14*, 5068-5076.

[56] Lee, J. C.; Gray, H. B.; Winkler, J. R. *J. Am. Chem. Soc.* **2008**, *130*, 6898-6899.

[57] Binolfi, A.; Rasia, R. M.; Bertoncini, C. W.; Ceolin, M.; Zweckstetter, M.; Griesinger, C.; Jovin, T. M.; Fernàndez, C. O. *J. Am. Chem. Soc.* **2006**, *128*, 9893-9901.

[58] Camponeschi, F.; Valensin, D.; Tessari, I.; Bubacco, L.; Dell'Acqua, S.; Casella, L.; Monzani, E.; Gaggelli, E.; Valensin, G. *Inorg. Chem.* **2013**, *52*, 1358-1367.

[59] Zawisza, I.; Rozga, M.; Bal, W. *Coord. Chem. Rev.* **2012**, *256*, 2297-2307.

[60] Moriarty, G. M.; Minetti, C. A.; Remeta, D. P.; Baum, J. *Biochemistry* **2014**, *53*, 2815-2817.

[61] Migliorini, C.; Porciatti, E.; Luczkowski, M.; Valensin, D. *Coord. Chem. Rev.* **2012**, *256*, 352-368.

[62] De Ricco, R.; Potocki, S.; Kozlowski, H.; Valensin, D. *Coord. Chem. Rev.* **2014**, *269*, 1-12.

[63] Savitzky, A.; Golay, M. J. E. *Anal. Chem.* **1964**, *36*, 1627–1639.

[64] Keller, R.; Wuthrich, K. Computer-aided resonance assignment (CARA). http://www.nmr.ch.

[65] Hwang, T. L.; Shaka, A. J. *J. Magn. Res.* **1995**, *112*, 275–279.

[66] Pascarella, S.; Milpetz, F.; Argos, P. *Protein Eng.* **1996**, *9*, 249-251.

[67] Ravel, B.; Newville, M. *J. Synchrotron. Rad.* **2005**, *12*, 537-541.

[68] Tomic, S.; Searl, B. G.; Wander, A.; Harrison, N. M.; Dent, A. J.; Mosselmans, J. F. W.; Inglesfield, J. E. New Tools for the Analysis of EXAFS: The DL EXCURV Package CCLRC Technical Report DL-TR-2005-001, ISSN 1362-0207.

[69] Binsted, N. EXCURV98: CCLRC Daresbury Laboratory computer program, **1998**.

[70] Whittle, P. J.; Blundell, T. L. *Annu. Rev. Biophys. Biomol. Struct.* **1994**, *23*, 349-375.

[71] Guntert, P.; Mumenthaler, C.; Wutthrich, K.; *J. Mol. Biol.* **1997**, *273*, 283-298.

[72] Koradi, R.; Billeter, M.; Wüthrich, K. *J. Mol. Graph.* **1996**, *14*, 51–55.

[73] Pickering, I. J.; George, G. N.; Dameron, C. T.; Kurz, B.; Winge, D. R.; Dance, I. G. *J. Am. Chem. Soc.* **1993**, *115*, 9498-9505.

[74] Chauhan, S.; Kline, C. D.; Mayfield, M.; Blackburn, N. J. *Biochemistry* **2014**, *53*, 1069-1080.

[75] Himes, R. A.; Park, G. Y.; Barry, A. N.; Blackburn, N. J.; Karlin, K. D. *J. Am. Chem. Soc.* **2007**, *129*, 5352-5353.

[76] Himes, R. A.; Park, G. Y.; Siluvai, G. S.; Blackburn, N. J.; Karlin, K. D. *Angew. Chem. Int. Ed.* **2008**, *47*, 9084-9087.

[77] Jullien, A. S.; Gateau, C.; Kieffer, I.; Testemale, D.; Delangle, P. *Inorg. Chem.* **2013**, *52*, 9954-9961.

[78] Kau, L. S.; Spira-Solomon, D. J.; Penner-Hahn, J. E.; Hodgson, K. O.; Solomon, E. I. *J. Am. Chem. Soc.* **1987**, *109*, 6433-6442.

[79] Banci, L.; Bertini, I., Mangani, S. *J Synchrotron Radiat.* **2005**, *12*, 94-97.

[80] Faller, P.; Hureau, C.; Berthoumieu, O. *Inorg. Chem.* **2013**, *52*, 12193-12206.

[81] Miotto, M. C.; Rodriguez, E. E.; Valiente-Gabioud, A. A.; Torres-Monserrat, V.; Binolfi, A.; Quintanar, L.; Zweckstetter, M.; Griesinger, C.; Fernández, C. O. *Inorg. Chem.* **2014**, *53*, 4350-4358.

1
2
3
4
5
6
7
8
9
10
11
12
13
14
15
16
17
18
19
20
21
22
23
24
25
26
27
28
29
30
31
32
33
34
35
36
37
38
39
40
41
42
43
44
45
46
47
48
49
50
51
52
53
54
55
56
57
58
59
60
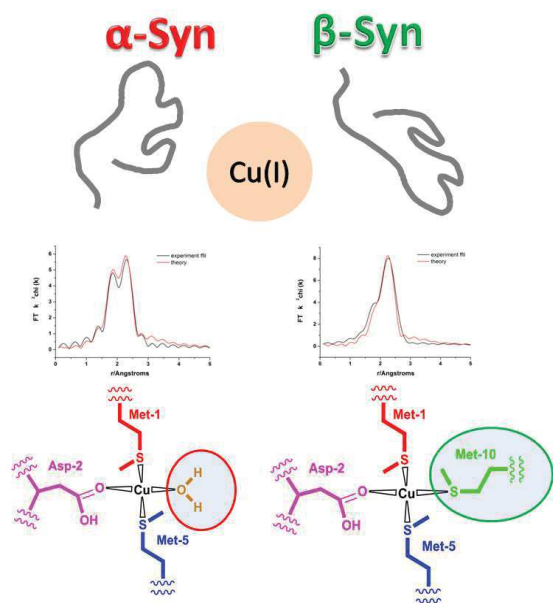
Spectroscopic Investigations of the interaction of Cu(I) with the N-terminal region of α- and β-synucleins.